

***Extracting short-ranged interactions from structure factors***

A.A. Louis\*

*Rudolf Peierls Centre for Theoretical Physics, 1 Keble Road, Oxford OX1 3NP, England*  
(Received 00 Month 200x; final version received 00 Month 200x)

Inverting scattering experiments to obtain effective interparticle interactions is generally a poorly conditioned problem. L. Reatto (Phil. Mag. A **58**, 37 (1986)) showed that for atomic liquids close to the triple point, inversions are hard because the structure closely resembles that of an equivalent hard-sphere fluid. Here I demonstrate that at low concentrations and for particles with short-ranged attractive potentials,  $S(k)$  also exhibits a very weak dependence on potential shape. Instead, different potentials all generate an  $S(k)$  that closely resembles that of the Baxter model with a similar second-virial coefficient. By contrast, in this energetic fluid regime, the inversion of an attractive interaction from real-space correlations such as the radial distribution function  $g(r)$  is well conditioned. Nevertheless, one may extract further information from  $S(k)$  by measuring *isosbestic points*, values of  $k$  where the scattering intensity  $I(k)$  or the structure factor  $S(k)$  is invariant to changes in interaction-potential well-depth. These points suggest a new extended corresponding states principle for particles in solution based on the packing fraction, the second osmotic virial coefficient, and a new measure of effective potential range.

**Keywords:** short ranged potentials, structure factors, Baxter model

**1. Introduction**

Extracting effective interparticle interactions from experiments is a central objective in chemical physics because these interactions govern physical behaviour [1]. But like many such inverse problems, this task is complicated. Experimental data is not perfect: statistical fluctuations occur, and results may not be obtainable over a complete parameter range. Moreover, the inversion procedures are often ill conditioned: small differences in the initial input can result in large changes in the final output.

This article concentrates on the determination of (spherically symmetric) effective interparticle pair potentials  $v^{eff}(r)$  from experimental scattering data for particles in solution. This problem is related to better studied question of how to obtain interatomic potentials from liquid state structure factors  $S(k)$  for simple liquids, where the need for very accurate experimental data, and sophisticated predictor-corrector inversion schemes [2] is firmly established. For simple liquids, inversions are subtle in part because the structure is dominated by their hard-cores [3]. For example, the  $S(k)$  for monotonic atomic liquids are almost quantitatively approximated by those of hard spheres (HS) [3, 4] so that the attractive interactions can only be determined by measurements accurate enough to distinguish the small deviations from HS like behaviour.

For particles in solution, the range of relevant effective volume fractions  $\eta$  is larger than in the better studied case of simple liquids near the triple point. In particular,

---

\*Corresponding author. Email: ard.louis@physics.ox.ac.uk

volume fractions are often much lower than those that lead to an entropy dominated freezing transition. At these lower volume fractions, and for short-range attractive interactions, the real-space structure can be dominated by the attractions, so that one can speak of *energetic fluids* [5]. Extraction of effective interactions from real-space measurements of the pair-correlation function  $g(r)$  is a well-conditioned problem for energetic fluids [6]. However, real-space measurements are not always possible or available. In this article I will show that inversions from  $S(k)$  are as problematic for energetic fluids as they are for entropic fluids, albeit for different reasons. These problems can be partially circumvented by studying *isobestic points* – values of the wave-vector  $k$  for which  $S(k)$  is invariant under changes of the attractive potential well depth. Isobestic points can be used to determine the effective range of the  $v^{eff}(r)$ , and also suggest an extended corresponding states principle for particles in solution, described by three experimentally accessible variables: the range defined by these points, the particle density  $\rho$  and the reduced second osmotic virial coefficient  $B_2^* = B_2/B_2^{HS}$ , where  $B_2^{HS}$  is the second virial coefficient of a hard-sphere (HS) system.

## 2. Inverting structure factors at low packing fractions

For particles in solution, the scattering intensity  $I(k)$ , measured by light, X-rays, or neutrons, is usually interpreted by dividing  $I(k)$  by the single particle form factor  $P(k)$ , to obtain the structure factor  $S(k) = I(k)/(\rho P(k))$  [7]; here  $\rho = N/V$  is the density. From  $S(k)$ , inferences can then be made about the form of the inter-particle interactions  $v^{eff}(r)$ .

Fig. 1 helps set the stage and introduce the problem to be addressed here. Experimental data [8], taken from small-angle neutron-scattering (SANS) of a microemulsion composed of small water droplets, coated with a layer of surfactant (AOT), is compared to some theoretical structure factors  $S(k)$ . In the original letter [8] a best fit, using an approximate integral equation technique, yielded a hard-core diameter of  $\sigma = 60\text{\AA}$ , a packing fraction  $\eta = \pi\sigma^3/6 = 0.075$ , and an attractive square well (SW) potential with a range  $\Delta_{SW} = 0.02\sigma$  and a well depth of  $\beta v(\sigma) = 3.85$ . The quality of the integral equation fit was then confirmed by independent computer simulations. However, as strikingly demonstrated by Fig. 1, a wide range of other potentials, depicted in Fig. 1(b), also lead to fits of similar accuracy. These include HSs with attractive SWs of two different ranges  $\Delta_{SW}$ , an Asakura-Oosawa (AO) depletion potential [9] of range  $\Delta_{AO}$ , an alternate simplified depletion potential of range  $\Delta_D$  showing the effects of solvation layers [10], as well as a Lennard-Jones- $n$  (LJ- $n$ ) potential, defined as:

$$v(r) = 4\epsilon \left( \left( \frac{\sigma}{r} \right)^{2n} - \left( \frac{\sigma}{r} \right)^n \right), \quad (1)$$

with  $n = 12$ . The  $S(k)$  are calculated within the Percus Yevick (PY) integral equation closure [3, 11], and are close to the analytical PY solution of Baxter's model [12].

Improving significantly on these pioneering experiments is hard.  $S(k)$  is obtained by dividing  $I(k)$  through by  $P(k)$ , which is only approximately determined, and which rapidly decays to zero for increasing  $k\sigma$ , so that achieving better accuracies for a larger  $k\sigma$  range is very difficult. As is clear from Fig. 1 (c), real-space measurements of  $g(r)$  would be much more sensitive to the effective potentials. Although increasingly accurate techniques being developed for the real-space measurement of the  $v^{eff}(r)$  of particles in solution [6, 13], these are often limited to certain particle

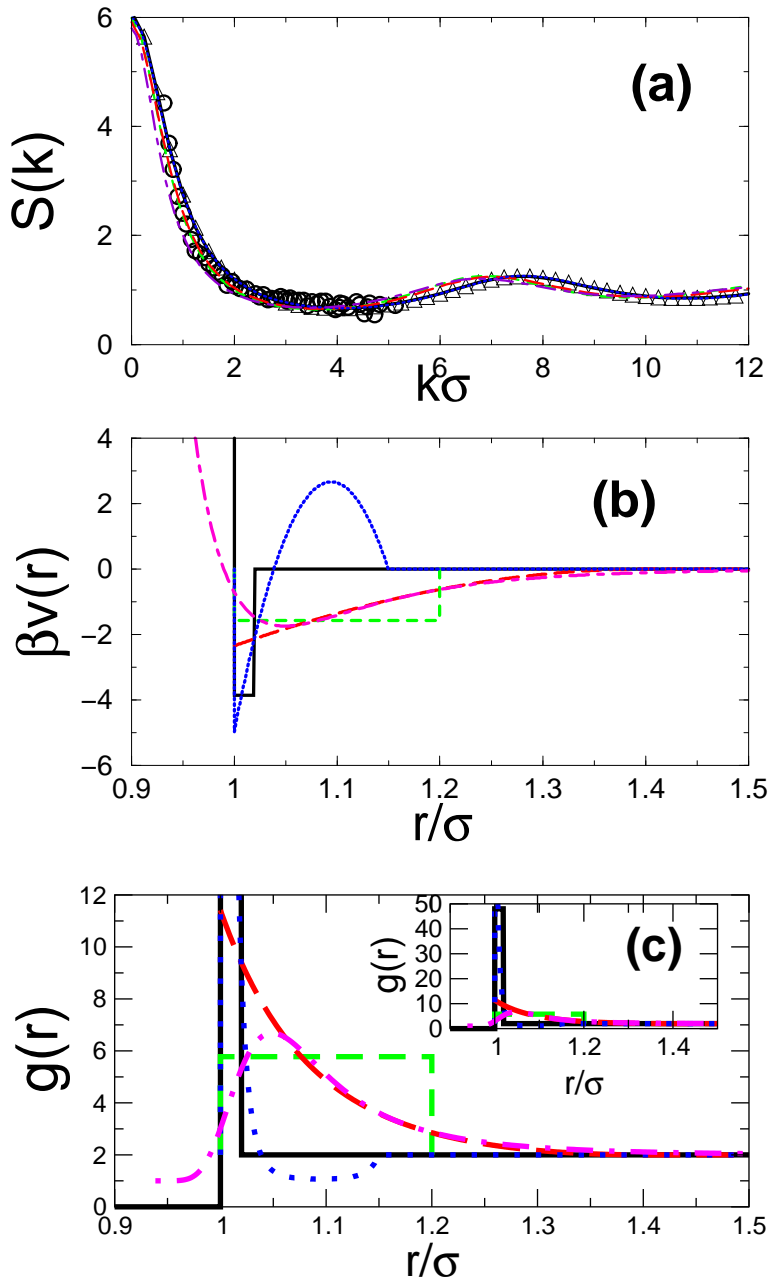


Figure 1. (colour online) A single set of experimental data can be interpreted by many different effective potentials. (a) The experimental SANS data (circles) on a microemulsion at packing fraction  $\eta = 0.075$  is from [8]. The open triangles denote the  $S(k)$  from the Baxter model [12] for  $B_2^* = -1.60$ , while the other  $S(k)$  are calculated for the potentials shown in (b). These include SWs with  $\Delta_{SW} = 0.02$  (solid lines) and  $\Delta_{SW} = 0.2$  (dashed), an AO form with  $\Delta_{AO} = 0.4$  (long-dashed), a generalised depletion form with  $\Delta_D = 0.2$  (dotted) and a LJ-12 (dot-dashed) potential. (c) The radial distribution function  $g(r)$  is much more sensitive to the potentials in this energetic fluid regime than the  $S(k)$  is. The line-styles in the three graphs correspond with each other.

types or sizes. The microemulsion measured in [8], for example, would be hard to characterise by current real-space techniques

The upshot of Fig. 1 is that deducing an effective potential from experimental scattering data at one state point is difficult; the inversion is ill-conditioned. Clearly more information is needed to interpret the data [14].

But first, what can be inferred from a single  $S(k)$ ? One hint comes the Baxter model, which is completely determined by the packing fraction  $\eta$  and the reduced osmotic virial coefficient  $B_2^*$  or equivalently, the Baxter parameter, defined as  $\tau =$

$\frac{1}{4}/(1 - B_2^*)$ . The  $S(k)$  in Fig. 1, with effective  $\tau$  parameters ranging from  $\tau = 0.093$  to  $\tau = 0.10$  are all close to the Baxter model result with  $\tau = 0.096$ . To first order therefore, measuring a single  $S(k)$  in this regime of low packing fraction, commonly encountered for particles in solution, does not result in much more information about the effective potential than the reduced second virial coefficient  $B_2^*$ . Just as found for simple liquids, where inversions are hard because the  $S(k)$  resemble those of HS fluids [3], here difficulties arise because they are close to the Baxter  $S(k)$ . Distinguishing between different potentials will only be possible by measuring deviations from the Baxter model, and these may be very small at any one statepoint.

### 3. Isosbestic points in structure factors

To make further progress, measurements at other state points are necessary. This is done in Figs. 2(a)-(d), which depict the  $S(k)$  calculated for four LJ- $n$  potentials at different temperatures. A best fit to the Baxter model  $S(k)$  at each temperature would result in  $B_2^*$  as a function of temperature. But there is clearly more information in these curves: Each of the four  $v^{eff}(r)$  results in a different set of *isosbestic points*, where the  $S(k)$  is invariant for different temperatures. Fig. 2(e) shows that the first isosbestic point  $k_1\sigma$  increases with increasing  $n$ , reflecting the decrease of the range of the LJ- $n$  potential (1) depicted in Fig. 2(f). (Error bars in Fig 2(e) reflect the approximate nature of the isosbestic points.)

These observations can be quite easily rationalised by the following simple theory: If the total correlation function  $h(r) = g(r) - 1$  is split into two parts, with  $h_0(r) = -1$  for  $r < \sigma$ , and  $h_1(r) = g(r) - 1$  for  $r \geq \sigma$ , then the structure factor  $S(k) = 1 + \rho\hat{h}(k)$  simplifies to

$$S(k) = 1 + \frac{4\pi\rho}{k}j_1(k) + \rho\hat{h}_1(k), \quad (2)$$

where  $j_1(k)$  is the first spherical Bessel function, and  $\hat{h}_1(k)$  is the Fourier Transform (FT) of  $h_1(r)$ . For potentials with a hard-core, such as most of those depicted in Fig. 1(b), this is exact, but even for the LJ- $n$  potentials this is a good approximation [15]. Since  $\hat{h}_0(k) = \frac{4\pi\rho}{k}j_1(k)$  is independent of temperature (barring small effective  $\sigma$  effects), Eq. 2 suggests that isosbestic points occur whenever  $\hat{h}_1(k) = 0$ . We note that a similar derivation was made within the MSA approximation by Tuinier and Vliegthart [16], who showed that isosbestic points may also occur for longer ranged potentials.

It has already been pointed out that in many experimentally relevant cases with low  $\eta$ , the  $g(r)$  are surprisingly well approximated by a simple form  $g(r) = \exp(-\beta v(r))$  [5], as explicitly demonstrated in Fig. 3. This simple approximation, equivalent to taking a Mayer function [3] for  $h(r)$ , works best for particles with short range attractive potentials. These can become quite deep, leading to large values of  $g(r)$  near contact, well before the system crosses a liquid-liquid or liquid-solid phase-line. Within this approximation, the dominant effect of varying the temperature is to change the amplitude of  $h_1(r)$  (as demonstrated in Fig. 3(b)). To first order, the period of  $\hat{h}_1(k)$  is not affected and each  $k\sigma$  where  $\hat{h}_1(k) = 0$  leads to an isosbestic point. For an infinitely narrow potential, the isosbestic points would be at  $k_n\sigma = n\pi$ , but for a finite potential range there is a phase-shift, which explains why the  $k_n\sigma$  move progressively further from  $n\pi$  with increasing range. The excellent accuracy of this simple Mayer function theory for the first isosbestic point

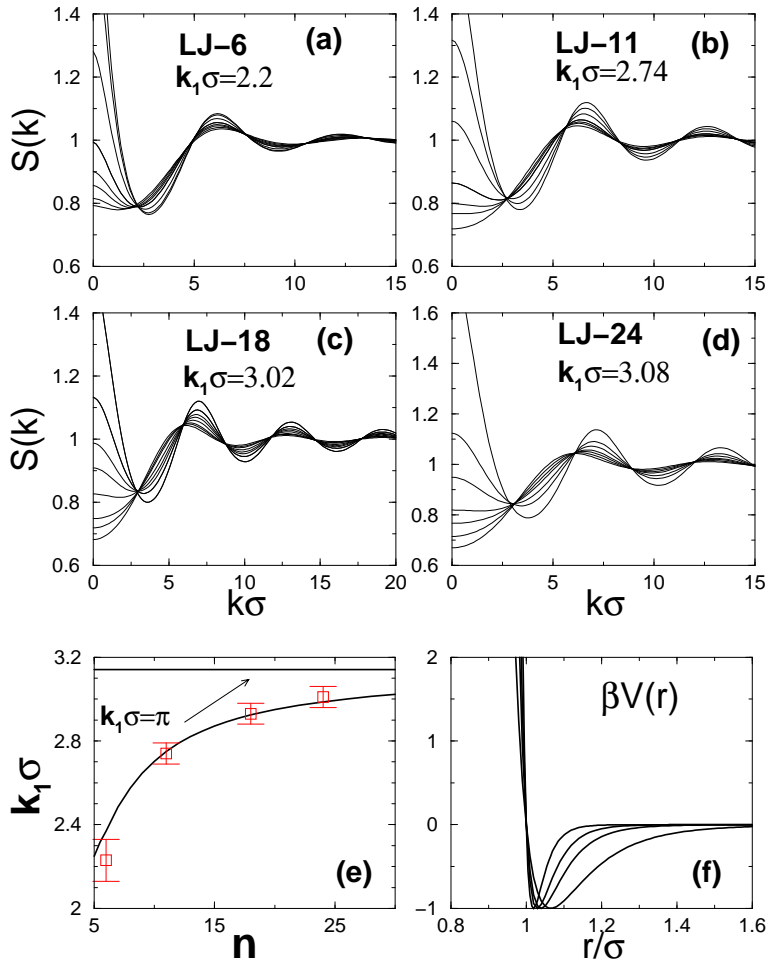


Figure 2. (colour online) (a)-(d)  $S(k)$  were calculated at  $\eta = 0.0576$  and at different temperatures for each of the four LJ- $n$  potentials  $v^{eff}(r)$  given by Eq. (1). Different  $v^{eff}(r)$  lead to different isosbestic points  $k_n\sigma$ . (e) The first isosbestic point  $k_1\sigma$  approaches  $\pi$  with increasing  $n$ . A simple theory (solid line), described in the text, fits the data well. (f) The range of the LJ- $n$  potentials in (a)-(d) decreases with increasing  $n$ .

$k_1\sigma$  is demonstrated by the solid line in Fig. 2(e).

The examples depicted in Fig. 2 are at a relatively low packing fraction, but the isosbestic points are robust up to packing fractions of at least  $\eta = 0.2$ , as shown in Fig. 4(a) [17]. These points are accurately described by the simple theory, described above.

Effective potentials in complex fluids may have many origins [1], so that one cannot simply vary the temperature to change the well depth. Nevertheless, the analysis above suggests that if varying a parameter leads to isosbestic points, then it is possible that the well-depth of  $v^{eff}(r)$  is changing while the range is not. When combined with the variation of  $B_2$ , this can help fix the form of  $v^{eff}(r)$ . However, this information may still not be sufficient, since the well-depth of  $v^{eff}(r)$  may depend in an (unknown) non-linear fashion on the parameters like the temperature  $T$ , the pH, and salt or other additive concentration. Furthermore, as shown in Fig. 4(b), different potential shapes, picked to have the same isosbestic points, can generate similar  $S(k)$  for each value of  $B_2^*$ .

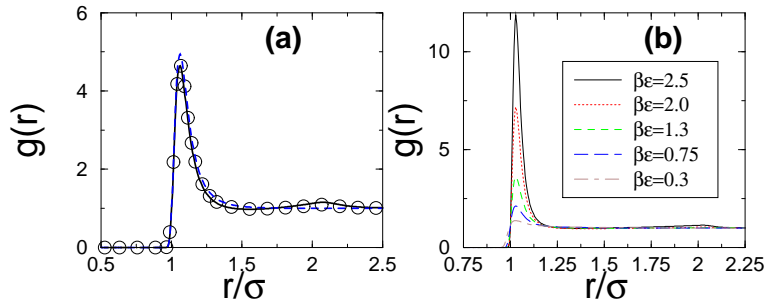


Figure 3. (colour online) (a) The PY approximation (solid line) very accurately reproduces these molecular dynamics simulations [11] of a LJ-12 potential at  $\beta\epsilon = 1.6$ , and  $\eta = 0.1$ . The simpler  $g(r) = \exp(-\beta v(r))$  form (dashed lines) is also accurate. (b) When the temperature is changed, the dominant effect on  $g(r)$ , calculated here with PY, is to change its amplitude.

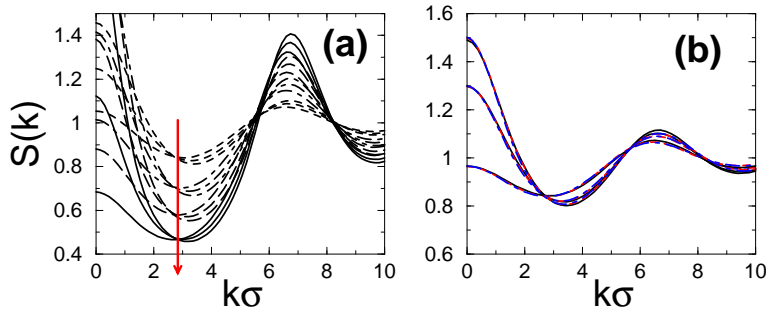


Figure 4. (colour online) Fig (a) The position of isobestic points barely varies with density for LJ-12, shown here for three temperatures  $\beta\epsilon = 1.5, 1.33, 1.09$  at each density  $\eta = 0.05, 0.1, 0.15, 0.2$ . The line with the arrow denotes  $k_1\sigma$  for increasing  $\eta$ . (b) Three potentials leading to the same isobestic points: SW ( $\Delta_{SW} = 0.26$ ) (solid lines), AO ( $\Delta_{AO} = 0.6$ ) (dashed lines) and LJ-22 (dot-dashed lines) for  $\eta = 0.05$  and  $B_2^* = 0, -0.719, -1$  (plots in descending order of  $B_2$  at  $k = 0$ ).

#### 4. An extended corresponding states principle

This similarity of the  $S(k)$  ties in with the work of Noro and Frenkel (NF), who proposed that many properties of particles in solution could be understood from an extended corresponding state principle based on the variables  $\eta$ ,  $B_2^*$ , and an effective well depth  $\beta\epsilon$  [18]. However, the three potentials shown in Fig. 4(b) do not have the same well-depth, while still showing similar  $S(k)$ . This suggests an alternative corresponding states principle based on the variables  $\eta$ ,  $B_2^*$ , and an effective range  $\Delta_{eff}$  related to the isobestic points. In fact, as NF point out, the potential range is not always uniquely defined when comparing different  $v^{eff}(r)$ 's. They suggested a non-linear mapping based on  $B_2^*$  to derive an effective SW range for each potential they consider.

Here I define the effective range  $\Delta_{eff}$  of a given potential as being that of an equivalent SW fluid with the same same  $k_1\sigma$ . A simple and accurate approximation of  $k_1\sigma$  for the SW fluid at low concentrations is given by  $k_1\sigma \approx \pi / (1 + \Delta_{eff}/2 + \Delta_{eff}^2/12)$  which follows from an expansion of the exact solution to the simple theory of isobestic points. Thus the value of the effective range is then well approximated by:

$$\Delta_{eff} = 24 \left( \frac{\pi}{3k_1\sigma} - \frac{1}{12} \right)^{\frac{1}{2}} - 12. \quad (3)$$

By comparing the  $k_1\sigma$  values for different potentials, some simple empirical rules

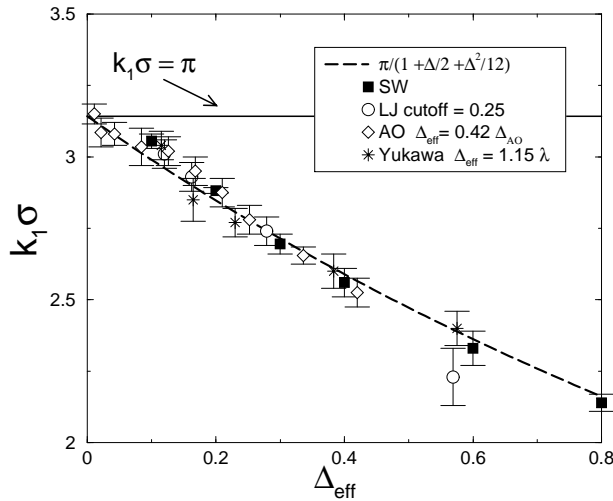


Figure 5. Defining effective range parameters from isosbestic points. For each potential type a simple mapping described in the text was used to derive an effective square well range  $\Delta_{eff}$ . For each potential, a PY calculation was used to find the isosbestic points, and these are shown in the plot for four different kinds of potentials. The long-dashed line denotes an accurate analytical approximation for the isosbestic points of square-well fluids. If one does not know what the potential is, then  $\Delta_{eff}$  can be directly estimated from the  $k_1\sigma$  measured in experiments.

can be derived: For the LJ-n potentials this criterion reduces to the distance  $r - \sigma$  where  $\beta v(r)$  reaches 1/4 of its maximum depth, for the AO potential the effective SW range is  $\Delta_{eff} \simeq 0.42\Delta_{AO}$ , and for the hard-core Yukawa potential, with an attractive tail of the form  $v(r) = \epsilon \exp(-r/\lambda)$  for  $r > \sigma$ , the mapping is  $\Delta_{eff} \simeq 1.15\lambda$ . The results are depicted in Fig. 5, and show that these simple linear mappings successfully define an effective range for each potential type.

Another argument for including the  $\Delta_{eff}$  (instead of the well-depth) as one of the relevant 3 variables is that the range determines the topology of the phase-diagram [18]. The critical range below which the fluid-fluid transition becomes metastable to the fluid-solid line is at  $\Delta_{eff} \approx 0.15$  for all four potentials (SW, AO, Yukawa and LJ-n), something consistent with what NF found. In addition,  $\Delta_{eff}$  is directly experimentally accessible through  $k_1\sigma$ . For example, taking advantage of the proximity of a metastable fluid-fluid critical point to enhance nucleation, a proposal made for protein solutions [19], would involve tailoring solution conditions such that the measured isosbestic point is just above  $k_1\sigma = 2.92$ , so that  $\Delta_{eff}$  is just below 0.15.

## 5. Discussion

In summary then, extracting effective potentials  $v^{eff}(r)$  from  $S(k)$  at the lower packing fractions typically encountered for particles in solution is a poorly conditioned problem. Whereas in simple liquids the HS model describes the dominant features of the  $S(k)$ , here the Baxter model appears to be the fundamental underlying model for  $S(k)$  around which different attractive potentials only induce a mild perturbation. More information can be obtained by studying the isosbestic points, which help determine the range  $\Delta_{eff}$  of the potentials. Together with  $\eta$  and  $B_2^*$ ,  $\Delta_{eff}$  can be used to define an extended corresponding states principle. Particles in solution with similar values of these three parameters should have similar properties, such as the relative stability of the fluid-fluid and fluid-solid binodals. In other words, many solution properties could be deduced without having to actually invert to an explicit form of  $v^{eff}(r)$ .



Nevertheless, It should always be kept in mind that the effective pair potential that reproduces the structure, even though it is unique [20], may not be the same as the effective potential that reproduces certain thermodynamic properties. Such representability problems [21] are typically important when there are large three-body interactions, or when the underlying system has anisotropic interactions [22]. For systems with truly short-ranged potentials, one doesn't expect strong many-body effects. Nevertheless, anisotropic interactions may be common for colloidal suspensions. They lead to important deviations from spherically symmetric potentials [23–26], could lead to representability problems if a potential is inferred from inverting structure factors.

In addition, particles in solution are often polydisperse, an effect that has been ignored in the current analysis. Polydispersity can manifest in multiple properties, i.e. in the effective diameters as well as in the interaction strengths. Clearly this adds a different dimension of complexity, and it would be interesting to see how isosbestic points would be affected by polydispersity. Encouragingly, structure factors have been solved for polydispersity in systems like the Baxter model [27], so that progress may be expected on this front in the future.

Finally, numerous examples of isosbestic points in  $S(k)$  can be found in the literature, ranging from colloids with short-range sticky coats [28], to colloid-polymer mixtures [29], to globular proteins [30], to magnetic colloids [31] and to colloid-micelle mixtures [32]. Interestingly, these points should also appear in  $I(k)$ .

### Acknowledgements

The author is very pleased to contribute to this Special Issue of Molecular Physics dedicated to Professor Luciano Reatto in recognition of his important contributions to the field, and wishes him much success in the coming years. The author also thanks P. Bartlett, J. P. K. Doye for valuable discussions. He also thanks Remco Tuinier and Gerrit A. Vliegthart for sharing with him their independent discovery of isosbestic points in structure factors [16].

### References

- [1] C.N. Likos, Phys. Rep. **348**, 267 (2001).
- [2] L. Reatto, Phil. Mag. A **58**, 37 (1986); L. Reatto, D. Levesque, and J.J. Weis, Phys. Rev. A. **33**, 3451 (1986).
- [3] J.P. Hansen and I.R. McDonald, *Theory of Simple Liquids, 2nd Ed.* (Academic Press, London, 1986).
- [4] N.W. Ashcroft and J. Lekner Phys. Rev. **145**, 83 (1966).
- [5] A.A. Louis, Phil. Trans. Roy. Soc. A **359**, 939 (2001).
- [6] C. P. Royall, A. A. Louis, and H. Tanaka J. Chem. Phys. **127**, 044507 (2007).
- [7] R. J. Hunter, *Foundations of Colloid Science, 2nd Ed.* (Oxford University Press, Oxford 2001).
- [8] J.S. Huang, S.A. Safran, M.W. Kim, G.S. Grest, M. Kotlarchyk, and N. Quirke, Phys. Rev. Lett. **53**, 592 (1984).
- [9] S. Asakura and F. Oosawa, J. Polym. Sci., Polym. Symp. **33**, 183 (1958), A. Vrij, Pure Appl. Chem. **48**, 471 (1976).
- [10] B. Götzemann, R. Evans, and S. Dietrich, Phys. Rev. E **57**, 6785 (1998).
- [11] More sophisticated closures [3] could be used, but for the low  $\eta$  regime discussed here, the PY approximation is adequate. This is demonstrated in Fig. 3, where the  $g(r)$  from a molecular dynamics simulation, performed with the MOLDY code (K. Refson, Comput. Phys. Commun. **126**, 310 (2000)) on a box of 1024 atoms, is virtually indistinguishable from the PY result. Similar accuracy was found for other potentials and parameters, and confirms the findings of other authors (See e.g. K. Shukla and R. Rajagopalan, Mol. Phys. **81**, 1093 (1994); M. Dijkstra, J. Brader, and R. Evans *J. Phys.: Condens. Matter* **11**, 10079 (1999) and references therein.). Another reason I use the PY closure is to facilitate comparisons with the Baxter model [12], which is only solved within PY.
- [12] R.J. Baxter, J. Chem. Phys. **49**, 2770 (1968).
- [13] See e.g. J.N. Israelachvili, *Intermolecular and Surface Forces* (Academic Press, London, 1992),
- [14] I should add that this is not an implicit critique of ref [8], where other physical considerations were indeed used to infer the suggested short ranged potential.



- [15] There are several similar ways to define an effective  $\sigma_{eff}$  for a LJ-n potential, see e.g. [3]. A more careful analysis shows that for our examples, these don't differ much from  $\sigma$ , and have a marginal effect on the isosbestic points.
- [16] R. Tuinier and G. Vliegenthart, unpublished manuscript
- [17] The isosbestic points typically move to a marginally higher  $k$  with increasing  $\eta$ , an effect also seen for the Baxter model; this can be used for a small correction to isosbestic points.
- [18] M.G. Noro and D. Frenkel, J. Chem. Phys. **113**, 2941 (2000) (and references therein).
- [19] P.R. ten Wolde and D. Frenkel, Science **277**, 1973 (1997).
- [20] R. L. Henderson, Phys. Lett. A **49**, 197, (1974); J.T. Chayes and L. Chayes, J. Stat. Phys. **36**, 471 (1984).
- [21] A. A. Louis, J. Phys.: Condens. Matter **14**, 9187 (2002).
- [22] M. E. Johnson, T. Head-Gordon, A. A. Louis J. Chem. Phys. **126**, 144509 (2007).
- [23] E. Allahyarov, H. Löwen, J. P. Hansen, and A. A. Louis, Phys. Rev. E **67**, 051404 (2003).
- [24] E. G. Noya, C. Vega, J. P. K. Doye, A. A. Louis J. Chem. Phys. **127**, 054501 (2007).
- [25] F. Romano, E. Sanz and F. Sciortino, J. Chem. Phys. **132**, 184501 (2010).
- [26] E. Bianchi, R. Blaak, and C. N. Likos, Phys. Chem. Chem. Phys. **13**, 6397 (2011).
- [27] A. Gazzillo and A. Giacometti, J. Appl. Cryst. **36**, 832 (2003).
- [28] M. H. G. Duits, R. P. May, A. Vrij, and C. G. de Kruif, Langmuir **7**, 62 (1991).
- [29] X. Ye, T. Narayanan, P. Tong, and J.S. Huang, Phys. Rev. Lett. **76**, 4640 (1996).
- [30] A. Tardieu *et al* J. Crystal Growth **196**, 193 (1999).
- [31] E. Dubois, V. Cabuil, F. Boué, and R. Perzynski, J. Chem. Phys. **111**, 7147 (1999).
- [32] P. Bartlett, private communication.